Daylighting performance assessment of a split louver with parametrically incremental slat angles: Effect of slat shapes and PV glass transmittance

Muna Alsukkar [a,b], Mingke Hu [a,1,*], Mohammed Alkhater [a], Yuehong Su [a,1]

[a] *Department of Architecture and Built Environment, University of Nottingham, Nottingham NG7 2RD, UK*
[b] *Department of Architectural Engineering, The Hashemite University, P.O. Box (330127), Zarqa, 13133, Jordan*

ARTICLE INFO

ABSTRACT

Advanced shading systems, including light redirecting systems, may cause undesirable glare and affect the quality of the transmitted daylight. Therefore, it is important to integrate different building components, such as shading and glazing, to comprehensively assess daylighting performance and ensure a comfortable, luminous environment. This study proposes an advanced daylighting design based on a parametrically controlled split louver with reflective slats to redirect sunlight onto a ceiling and integrated PV glazing to control the illuminance levels. A special contoured slat design (retro shape) was evaluated and compared to different slat shapes (flat, curved, and oval) of the upper section. In addition, the effect of the PV glass transmittance (30 %, 50 %, and 70 %) on the daylighting performance was investigated. The daylight analysis was performed using Grasshopper software as a parametric tool to predict the daylighting performance through advanced dynamic metrics including Useful Daylight Illuminance (UDI), Daylight Glare Probability (DGP), and Illuminance Uniformity (Uo). It is found that the *retro*-shaped slat design can significantly improve the daylight distribution and level without using the common blind system for more than 90 % of the work plane area within the recommended acceptable UDI range (150 ~ 750 lx) for a longer period of the day (including the early morning and late afternoon). Furthermore, *retro*-shaped slats can improve the Uo throughout the space to achieve the recommended level (0.70), while PV glazing can reduce the risk of daylight glare.

1. Introduction

Solar energy, as the most important renewable energy source, is also known as clean and environmentally friendly, which meets the demand for energy consumption and enhances daylighting [1–3]. Daylight plays an important role in the visual comfort level of buildings and their energy efficiency [4,5]. The efficient use of sunlight through the window as a source of natural daylight increases building efficiency and occupant comfort [6]. Different daylight controls, such as advanced or smart windows, can be used to control the amount of daylight entering buildings [7–9]. Some simulation results also show that a photovoltaic (PV) window offers better daylighting performance than conventional double glazing and effectively reduces the possibility of glare [10–13]. Combining natural daylighting with existing renewable energy technologies such as building-integrated photovoltaics (BIPVs) would be a more efficient way to use solar energy for buildings [14–16]. Specifically, to regulate the daylight entering the indoor space and avoid

potential glare, the combination of PV and shading devices (PV-integrated shading devices, PVSDs) has been developed in recent years [1,10,11,13,17].

Daylighting systems can be static or dynamic elements located on or near a building's facade to collect and redirect daylight into the building to improve daylighting performance and save energy [18–20]. Using advanced daylight redirection systems, the demands for electrical lighting can be reduced, thereby reducing overall energy consumption [21]. Although these well-known daylighting systems can reflect sunlight into a deep-plan space, the reflected light over the ceiling is not always uniform or steady. Furthermore, they may have some drawbacks, such as time limitations for daylight provided, glare or excessive light risk, and high contrast of light, which may cause visual discomfort to occupants [22]. Several shading system combinations might be constructed to provide both solar shading and natural daylight optimization [23]. Among these, employing split louvers with two (upper and lower) sections to balance the functions of redirecting and shading is an

---
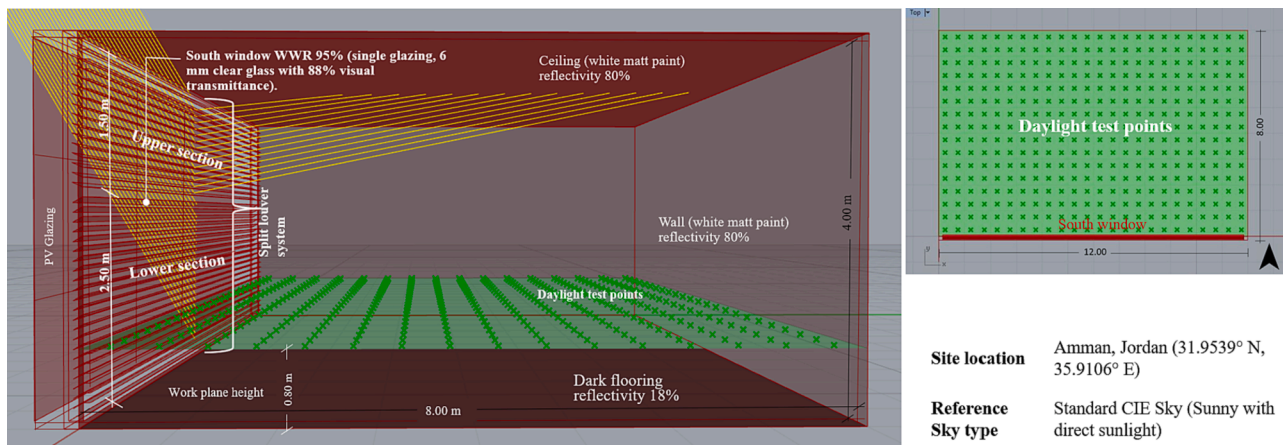
Fig. 1. Perspective view of a split louver in a virtual office room (left image) and top view with the daylight test points (right image).

effective strategy for better annual daylighting performance [5,24,25]. This parametric split louver, using both daylight redirecting and shading functions, helps enhance daylight distribution most of the time. However, control of the illuminance level and the inconsistency of daylight distribution in the early morning and late afternoon hours need to be highlighted. By adjusting the slat shape of the upper section of the split louver, it is possible to improve daylight uniformity during these periods [26].

The slat can be made in a variety of shapes to meet specific optical requirements, and many studies have been conducted to develop novel systems for this purpose [27–29]. Strategically modifying the slat's size and shape can result in improved performance when compared to the flat-shaped slat and its initial size [8,30]. Different macro and micro designs may transform a simple set of shades into a light-redirecting system that also controls heat and glare [31]. Yet, the exact shape (profile, layout, etc.) of more complex designs that parametrically respond to the solar angle has not been sufficiently investigated. Retro-shaped structures such as W- and V-shaped blinds, which can reflect excessive sunlight back into the sky, have been developed to reduce glare and overheating [32]. Furthermore, they can offer a slimmer profile in manufacturing and support sufficient visual transmission [18,22]. Therefore, a combination of advanced *retro*-shading devices and glazing is effective in ensuring overall visual comfort [33,34].

The present study aims to optimize the operation of PVSD technologies using transparent PV glass and an innovative *retro*-reflective slat design for split louvers. Building upon our prior work on split louvers with flat-shaped slats and standard window glazing [24,25], this research investigates the impact of parametric and geometric slat variations (cross-sectional profile) on daylighting performance. Additionally, the introduction of bifacial PV glazing and evaluation of various PV glass transmittance levels' effects on daylighting performance are addressed. The main objective is to achieve the maximum benefits of the split louver system for indoor daylighting performance by achieving steadier and more uniform daylight distribution during working hours in a deep-plan office room. A daylight model is developed in this study to characterise the daylighting performance of the proposed PV glazing-integrated split louver system with different slat shapes and PV glass transmittance values. This will serve as guidance for designing, manufacturing, and automatically regulating the split louver in real-world applications.

2. Materials and methods

2.1. Software and modelling

The present work employs the parametric software Grasshopper which is incorporated into the Rhinoceros 3D. Grasshopper is a graphical algorithmic editor capable of simultaneously controlling several parameters based on connected formulas. Grasshopper interface can insert different plugins such as "Honeybee and Ladybug", which can work as an engine to connect the well-known environmental software Radiance, Daysim, and EnergyPlus. The raytracing technology used by Radiance software allows it to effectively handle indirect diffuse light and caustics. Radiance can employ photon maps to recreate indirect lighting in volumes and comprehend complicated geometries with many surfaces and materials [35,36]. Ladybug is a gate that allows all weather data from any region to be accessed. In this study, annual hourly data analysis is generated for Alia International Airport in Amman, Jordan, applying climate-based hourly simulation and EPW weather file.

The application of Radiance for climate-based daylight modelling was initially documented by John Mardaljevic in 1995 [37], alongside comprehensive documentation and validation of its utility in calculating illuminance using daylight coefficients [38,39]. Originally designed to efficiently calculate illuminance across changing sky conditions, the daylight coefficient method has evolved by integrating multiple phases for flux transfer matrix computations between sensor points and discretized skies. This advancement aims to enhance calculation speed, augment spatial resolution, and enable the simulation of dynamic scenes [40]. Notably, for Complex Fenestration Systems (CFS) considering light transmission through fenestration, the framework grounded in the three-phase method enables precise parametric daylight simulations at specific time points [41]. This three-phase approach facilitates accurate annual daylight simulations in office spaces equipped with daylight redirecting components, offering an accurate spatial resolution that gives detailed insights into daylight distribution, as well as aiding in localized analysis and glare evaluation [40]. Additionally, its capability to accommodate dynamic scenes renders it suitable for investigating shading systems with dynamic characteristics. Nonetheless, effective utilization of the three-phase method necessitates computational resources, Radiance expertise, detailed input data, and simplifications in reflection assumptions, which might not accurately represent surfaces with high reflectivity [41]. Despite these considerations, the three-phase method confers advanced capabilities for precise and detailed daylight simulations, thereby enhancing our comprehension of lighting performance in built environments.

To attain accurate results in daylight simulations using Radiance, specific parameters need specification to consider the impacts of the model's surface materials, which warrants the inclusion of ambient values [42]. It is recommended to employ high-precision parameters for Radiance to ensure precise simulation outcomes, not solely for opaque materials but also for those with high reflectivity.

This study follows the determined scheduled angle for the split louver integrated blinds in our previous research [25] and the advanced louver system controlled parametrically to respond to the sun's

Table 1
The Radiance settings used in the simulation.

Radiance parameter	Description	Value
-aa	Ambient accuracy	0.2
-ab	Ambient bounces	3
-ad	Ambient divisions	2048
-ar	Ambient resolution	64
-as	Ambient super-samples	2048
-dr	Direct relays	1
-dp	Direct pretest density	256
-lw	Limit weight	0.01
-lr	Limit reflection	6
-st	Specular threshold	0.5

movement. The upper section, in conjunction with the lower section of the split louver, is used to balance the daylighting distribution. These slats in the upper section reflect the direct sunlight onto the ceiling of a deep-plan office room with 8 m depth and 12 m width, and then the illuminated ceiling acts as a light source for the room. It is important to note that the south window glazing is the common single glazing with an 88 % visual transmittance since this study involves the fully glazed façade with a 95 % window-to-wall ratio. The detailed model is described in Fig. 1. The upper and lower sections are respectively equipped with semi-mirrored slats (reflectivity 80 %, specularity 0.80, and roughness 0.05) and diffused slats (reflectivity 80 %, specularity 0.10, and roughness 0.10) with optimum parametric scheduled angles based on a previous study [25]. The walls and ceiling are matt white with a typical reflectivity of 80 %, while the flooring is a typical grey with a reflectivity of 18 %. Some Radiance parameters used in this simulation study are shown in Table 1 [42]. Honeybee (HB) simulation parameters such as analysis period, sky type, grid size, and Radiance rendering parameters are controlled parametrically. The main components of Radiance simulation, HB surfaces, CIE standard sky type, and Radiance parameters are connected to operate the grid-based daylight analysis using Radiance.

2.2. PV glazing-integrated split louver system

The proposed system essentially includes the main components of the split louver and PV glazing, with the additional component of common blinds. Including the scheduled parametric angle of the split louver, the main investigations of this study are slat shape and PV glass transparency.

2.2.1. Scheduled slat angles of the split louver system

The parametric method is applied to regulate the upper section, maximizing daylight benefits by redirecting sunlight according to spatial dimensions and location. Simultaneously, the lower section's slats control daylight near the window, working alongside the integrated PV glazing to balance quantity and quality. This design approach is depicted in Fig. 2. The split louver's two sections work together to balance daylighting levels and distribution throughout the space. Collaborating with the upper section, the lower section responds to the sun's movement and solar intensity. This study builds upon prior research regarding the scheduled slat angles for both sections, as well as the parametric incremental control of the upper section's slat angles, within the context of the studied model and "Amman, Jordan". The established split louver angle schedule for both sections represents optimal combinations for achieving balanced daylighting levels in both the front and back of the space, maintaining an acceptable daylight uniformity level of up to 0.6, and ensuring a high coverage percentage within the useful daylight illuminance (UDI$_{150\sim750\;lx}$) range, ranging from 90 % to 100 % at noontime and not falling below 50 % throughout the remaining working hours throughout the year [25].

2.2.2. Slat shape and geometry modifications

By carefully designing the shading slats, their geometries, surface characteristics, and levels of adjustability, it is possible to meet the desired daylighting performance even in some extreme cases with very low solar angles and intensities. It is essential to employ the louver slats' shape and their optical properties to maximise daylight utilization with well-managed and pleasant illuminance levels while minimising solar overheating and glare. The louver slats ensure that incident sunlight is redirected/reflected either into the depth of the room or back outside. The slats were considered flat in the previous analysis [24,25]. However, to explore the possibility of achieving further improvement in the daylighting performance of this split louver system, the present
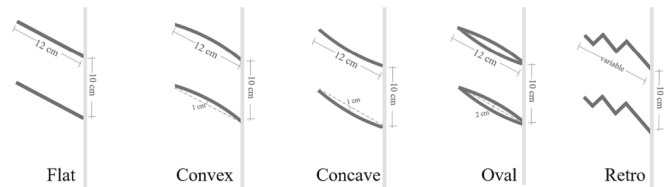
Fig. 3. Different slat shapes and their geometries.
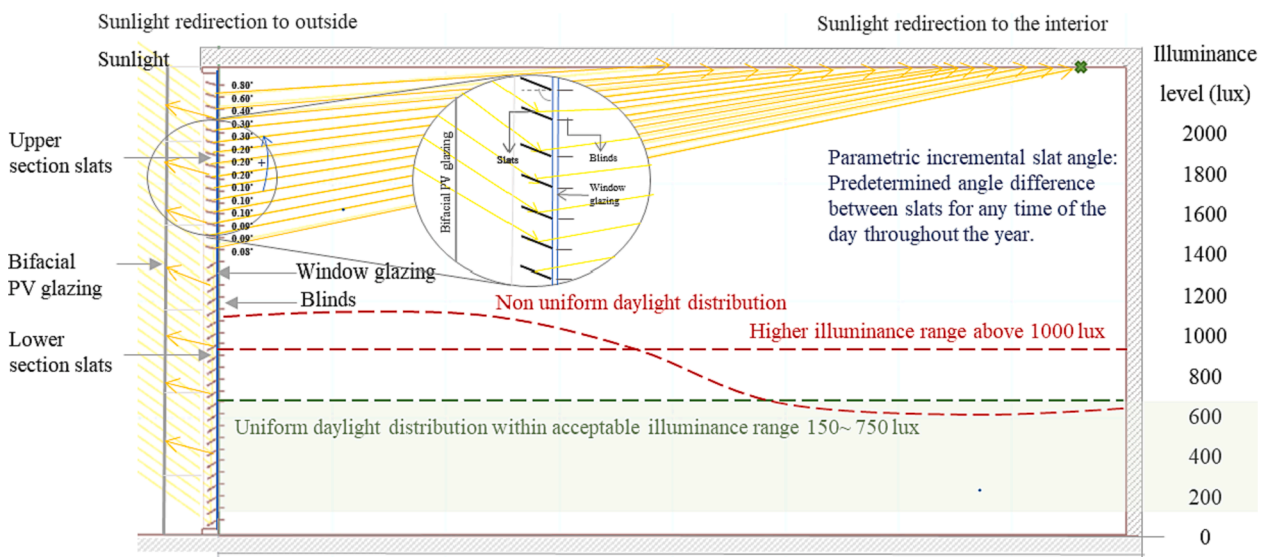
Fig. 2. The PV glazing-integrated split louver system.
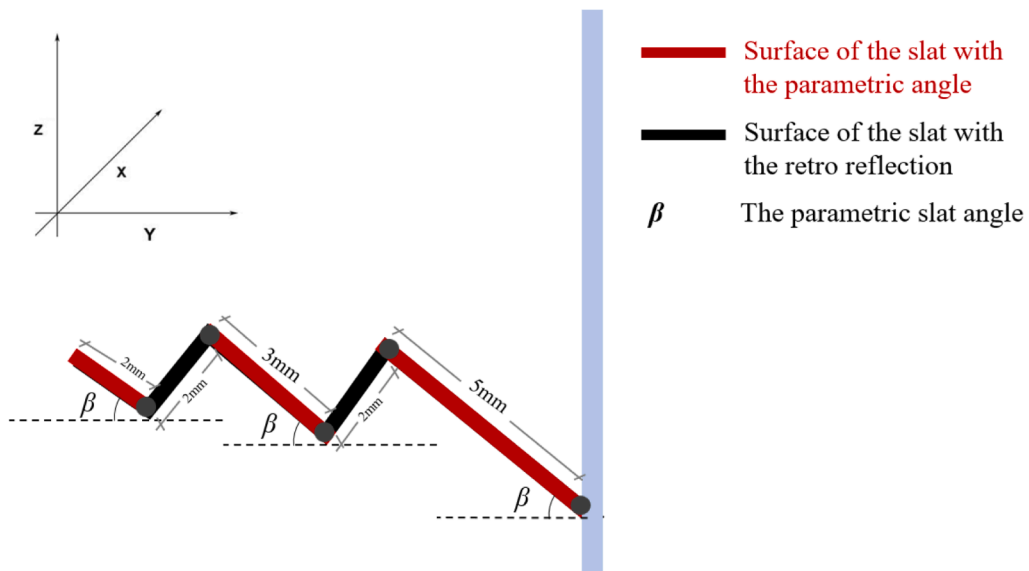
(a) Cross-section view (the red and black colours are only indicative)
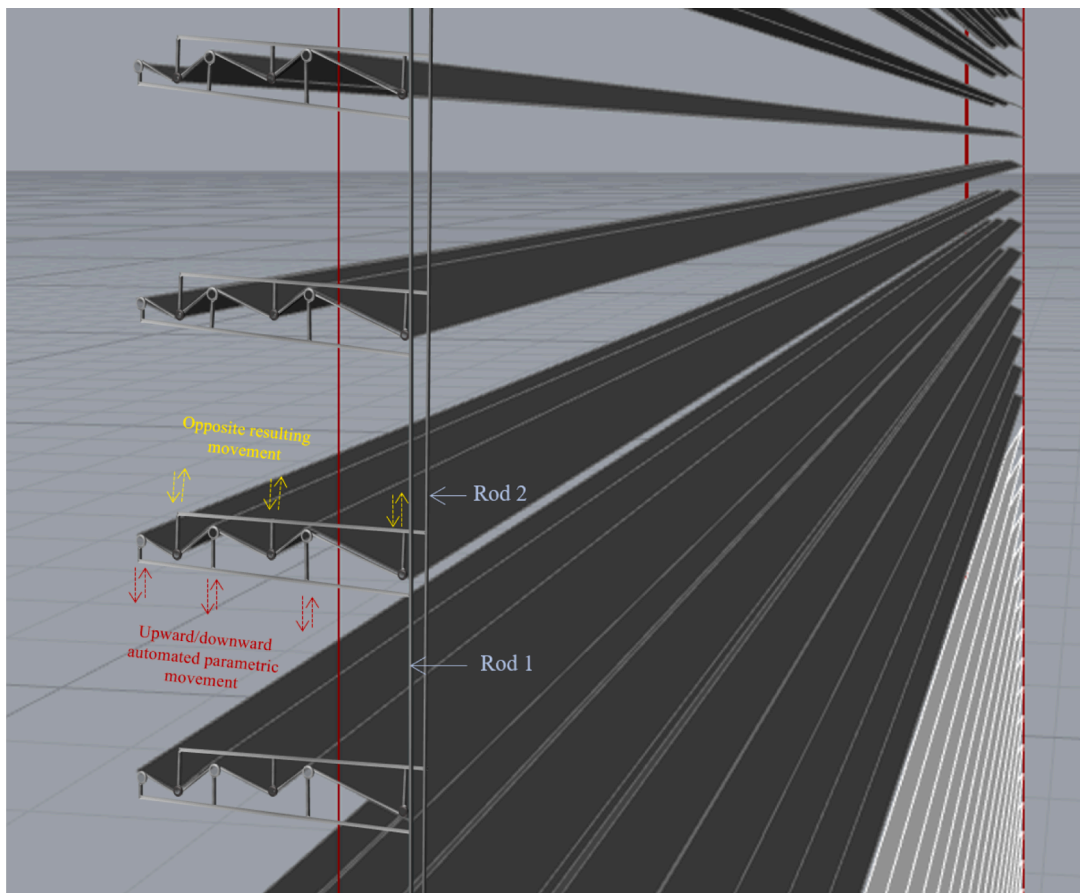
(b) 3D overall view with mechanical operation schematic of the retro-shaped slats

Fig. 4. Details of the slat with a special contoured shape (retro shape).

study investigates the performance of three surface slats (i.e., flat, concave, and convex slats), one body slat (i.e., oval slat), and a special contoured slat shape (i.e., retro slat), as shown in Fig. 3.

For the *retro*-shaped slats, each is divided into five fixed-length segments, where three critical angles are parametrically controlled to the same value (β), as shown in Fig. 4. The parametric angle (β) is assigned to the slat angle in three different slat segments that redirect the sunlight toward the ceiling. The other two segments face toward the PV glass. The tilt angle of the slats beyond which no direct sunlight can pass through adjacent slats is known as the "cut-off angle". The cut-off angle can be reached by changing the total length of the slat to its critical length, which is the horizontal distance between the start and
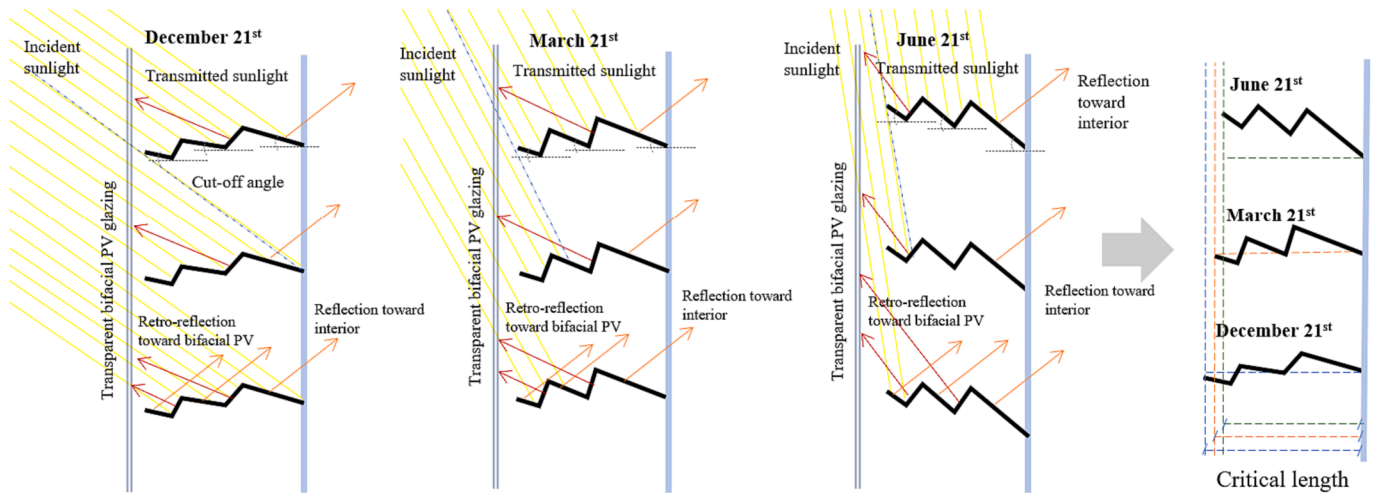
Fig. 5. The optimised *retro*-shaped slat for different seasons.
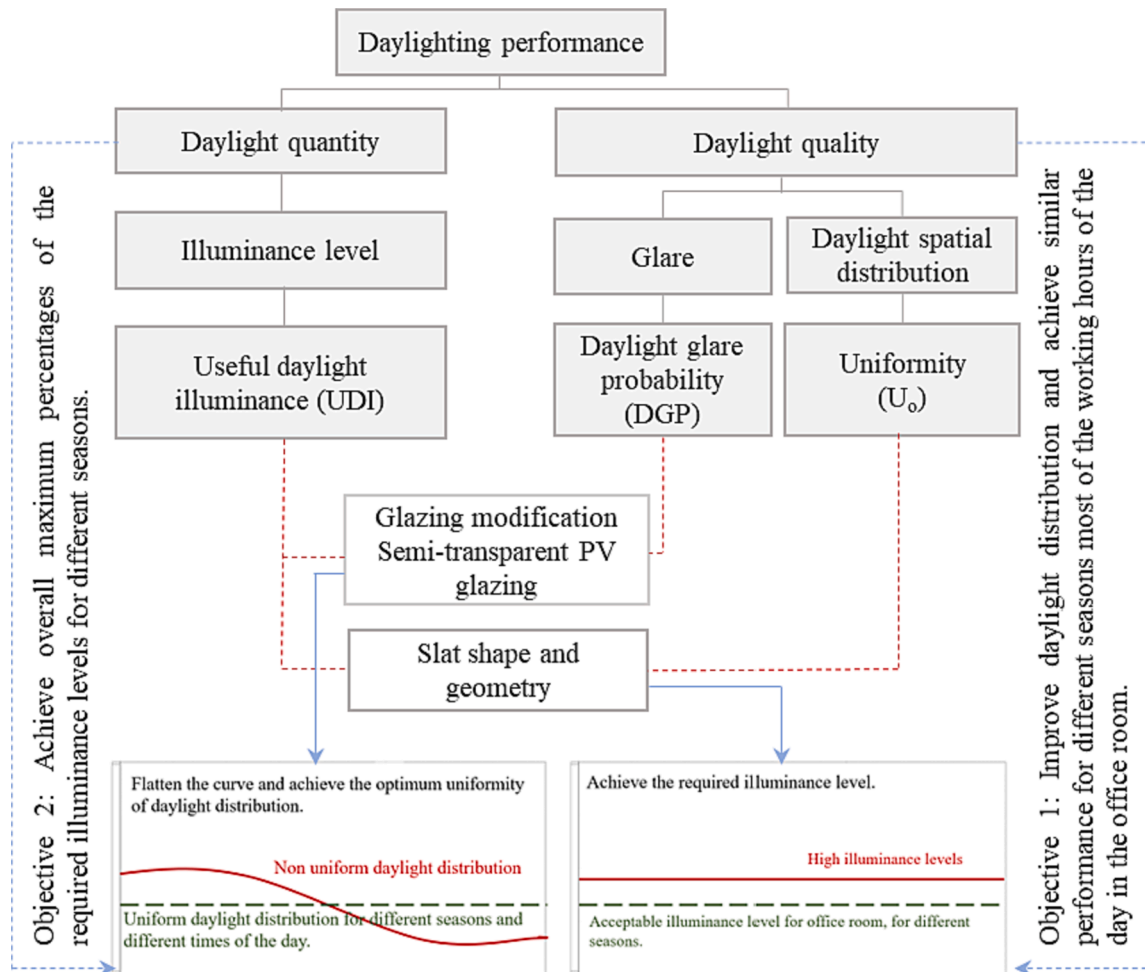
Fig. 6. Daylighting performance assessment of the PV glazing-integrated split louver system.

end points of the slat (see Fig. 5). In this study, the critical length of the slat is determined by the change of the β while the actual length of each segment remains constant. The slats are mechanically operated in a circular motion by five pivots, including the pivot attached to the window frame.

To follow the sun's movement, the slats in this system simultaneously rotate in one direction around their x-axis. This response aims to follow the sun wherever it moves and direct it to the ceiling. The *retro*-shaped slats are designed using the same mechanism for the three red segments in the same direction. Each slat segment has a hinge at one of its corners, allowing axial rotation around the x-pivot. The other corner of each segment, however, is set in a movable bar that can assist the slats' movement and achieve the critical length of slats that block any potential direct sun penetration.
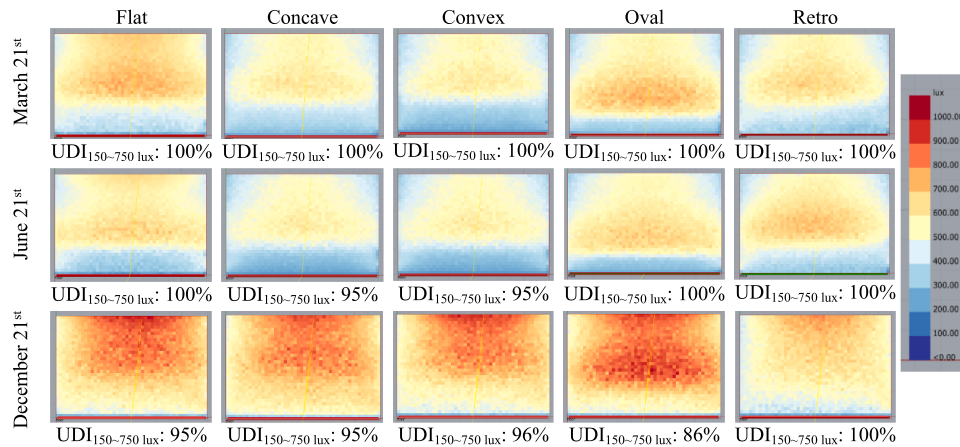
Fig. 7. Illuminance maps for different types of slats in the upper section of the split louver at 12:00 on three typical dates.

The fundamental idea is to direct the sun's reflected light toward predetermined target spots on the ceiling while steadily simultaneously (using *retro*-shaped slats) reflecting the undesirable light back to its source. At this point, the parametric software Grasshopper is in charge of controlling the slats' surfaces perpendicular to the sunbeam in order to reflect the sunlight to the ceiling in certain spots in accordance with the formula developed based on the solar angle and model dimensions. The red segments of the retro slats are designed to reflect the light toward the ceilings (the red segments in Fig. 4 simply need to be perpendicular to the sunbeam). This can be done by applying the same formula to determine the rotation angle of each segment in response to the sun using the same concept. On the other hand, the remaining black segments reflect the undesirable sun rays back to their source. The movement of these black segments is automatically linked to the movement of the red segments. Thus, the entire slat movement system is comprehensive, with all segments functioning based on a single variable, which is the three identical angles (β) of the *retro*-shaped slat.

A suggested method for the operation is illustrated in Fig. 4(b) to give an initial thought for the mechanical process of movement and control. Two rods will connect to the segment hinges. One rod (rod 1) will be connected to the hinge that moves downward or upward responding to the sun position, and the other rod (rod 2) will be connected to the remaining hinges that will forcefully have the opposite direction of the hinges that are connected to the first rod.

The *retro*-shaped design promotes effective daylighting and views while reducing glare and overheating. Specifically, it can offer a slimmer profile in manufacturing and support more visual transmission while simultaneously reflecting a part of incident sunlight to the PV glass for secondary electricity generation. Another benefit of *retro*-shaped slats is that they block penetrating direct or diffuse daylight without blinds, as discussed and analyzed later in this study.

2.2.3. PV glazing

PV windows function as a supplementary source of electric power to control the overall illuminance level inside the space. With thin-film incorporation in a glass-on-glass design, devices with up to 50 % transparency are commercially available. This technology allowed for a more uniform distribution of daylight throughout the interior spaces. However, the power conversion efficiency is connected to its visual transmittance [43,44]. As mentioned before, the PV glazing used in the proposed system is transparent bifacial PV glass installed vertically in front of the south façade window. A balanced solution between daylighting, solar heat gain, and electricity generation is needed [45]. Therefore, this work presents a quantitative assessment of illuminance distribution and glare using a PV glass with different transmittance values. The selected PV glass transmittance values (τ_{PV}) used in the simulation, namely, 30 %, 50 %, and 70 %, are based on PV availability

in the market. PV glass transmittance less than 30 % is not preferred in consideration of the visual requirement, and more than 70 % is not included considering the balance between PV cost and efficiency.

2.3. Daylighting performance assessment methods

The daylighting performance results obtained from Radiance and Daysim in the Grasshopper simulations of the system with modifications are evaluated using three metrics, as depicted in Fig. 6, to encompass both daylight quantity and quality. These metrics include useful daylight illuminance (UDI), daylight uniformity (Uo), and daylight glare probability (DGP).

Daylight quantity: Useful Daylight Illuminance (UDI)

UDI is a widely adopted dynamic metric for assessing daylight availability. The UDI range might vary based on design requirements, actual building use, and visual tasks [46,47]. In existing literature and standards, the illuminance levels of 150 lx and 750 lx were widely chosen as the lower and upper limits for daylighting analysis [25,46,48–50]. Therefore, the UDI range of 150 ~ 750 lx is chosen in this study as the daylight metric.

Daylight quality: Daylight spatial distribution and Glare (U_o and DGP*)*

U_o and DGP are metrics used to evaluate the daylight comfort level of the indoor space. U_o is used to represent the homogeneity of daylight distribution within a space and is determined by the minimum illuminance divided by the average illuminance [51] from the daylight study points. The suggested minimum value of uniformity is 0.40 [52] and the recommended value is 0.60 [53] from the daylight test points. DGP is selected for assessing discomfort glare using a glare check image in Grasshopper. Glare arises when the luminance within the field of view exceeds the maximum brightness to which the human eye can adapt [54]. The DGP results are divided into four bins: lower than 0.35 is an "imperceptible" glare sensation, between 0.35 and 0.40 is "perceptible", between 0.40 and 0.45 is "disturbing", and higher than 0.45 is considered "intolerable" [44,54]. A higher percentage of $UDI_{150\sim750\ lx}$, greater U_o, and minimum values of DGP in a room environment offer better visual comfort [55].

3. Comparison analysis and results

The daylighting performance comparisons are categorized into both quantity and quality analyses to explore distinct aspects of the PV glazing-integrated split louver with advanced modifications, focusing on (1) slat shape and (2) PV glass transparency. Since the incident sunlight conditions in the afternoon hours would be almost the same as the corresponding morning hours (for example, 8:00 vs. 16:00, 10:00 vs. 14:00) except for a different sun direction, only the daylighting performance of the split louver system at 8:00, 10:00, and 12:00 is
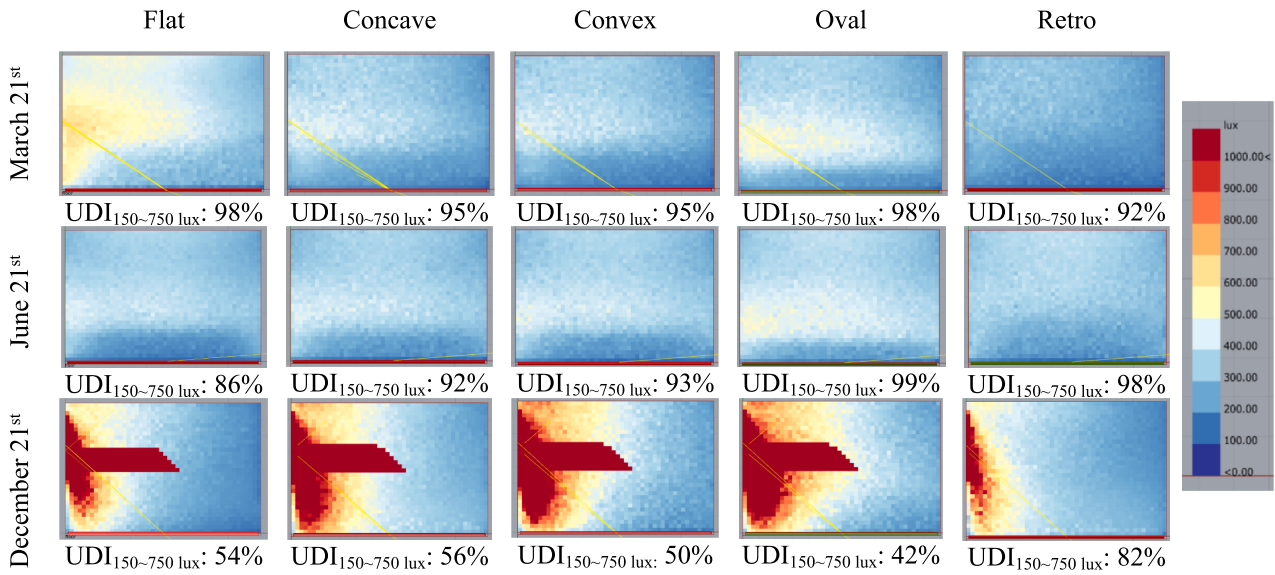
Fig. 8. Illuminance maps for different types of slats in the upper section of the split louver at 8:00 on three typical dates.
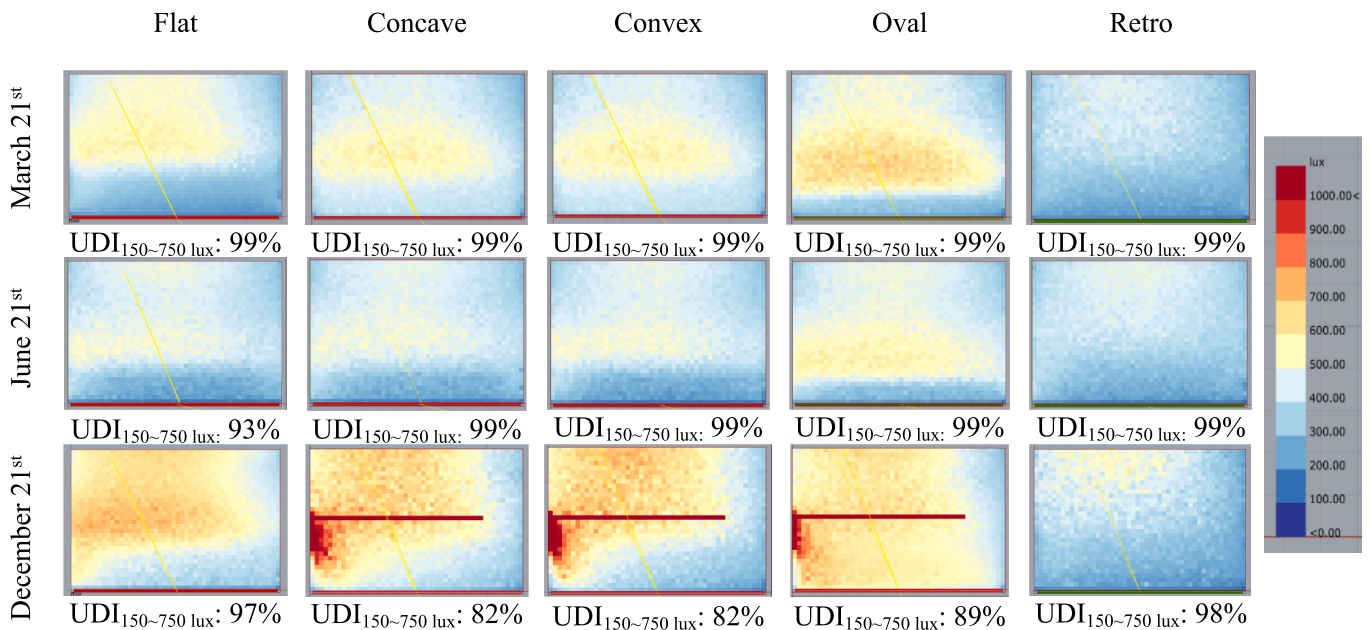
Fig. 9. Illuminance maps for different types of slats in the upper section of the split louver at 10:00 on three typical dates.

analyzed.

3.1. Daylight quantity analysis

The analysis of the daylight quantity investigates the split louver design and the integrated PV glazing in separate sections. The first analysis includes slat shape effects on useful daylight illuminance (UDI), midline lux distribution, and annual daylighting coverage percentage within $UDI_{150\sim750\ lx}$. The second section demonstrates the effect of PV glass transmittance on the illuminance along the midline and the percentage coverage of different UDI bins.

3.1.1. Effect of slat shapes
Based on the schedule angle of the split louver, different slat shapes (i.e., flat, concave, convex, oval, and retro) are involved in investigating the daylight availability performance through (1) illuminance

distribution maps, (2) average illuminance along the space midline, and (3) annual useful illuminance coverage percentages. In this section, no PV glazing is involved, and window glazing is common single glazing with 88 % visual transmittance.

Fig. 7 illustrates the illuminance distribution in the workspace for different slat shapes in the upper section of the split louver at 12:00 on three typical dates (i.e., March 21st, June 21st, and December 21st). The performance of the curved-shaped slats (convex and concave) is similar to that of the flat-shaped slat. In the case of the oval-shaped slat, the reflected light is slightly concentrated near the window, which causes undesirable daylight distribution on the three typical dates. On the contrary, the retro slat tends to distribute the reflected light in wider areas of the space, with higher percentages of $UDI_{150\sim750\ lx}$ on December 21st. In general, the daylighting performance is more similar for the three typical dates in the case of the *retro*-shaped slat, with 100 % of $UDI_{150\sim750\ lx}$.
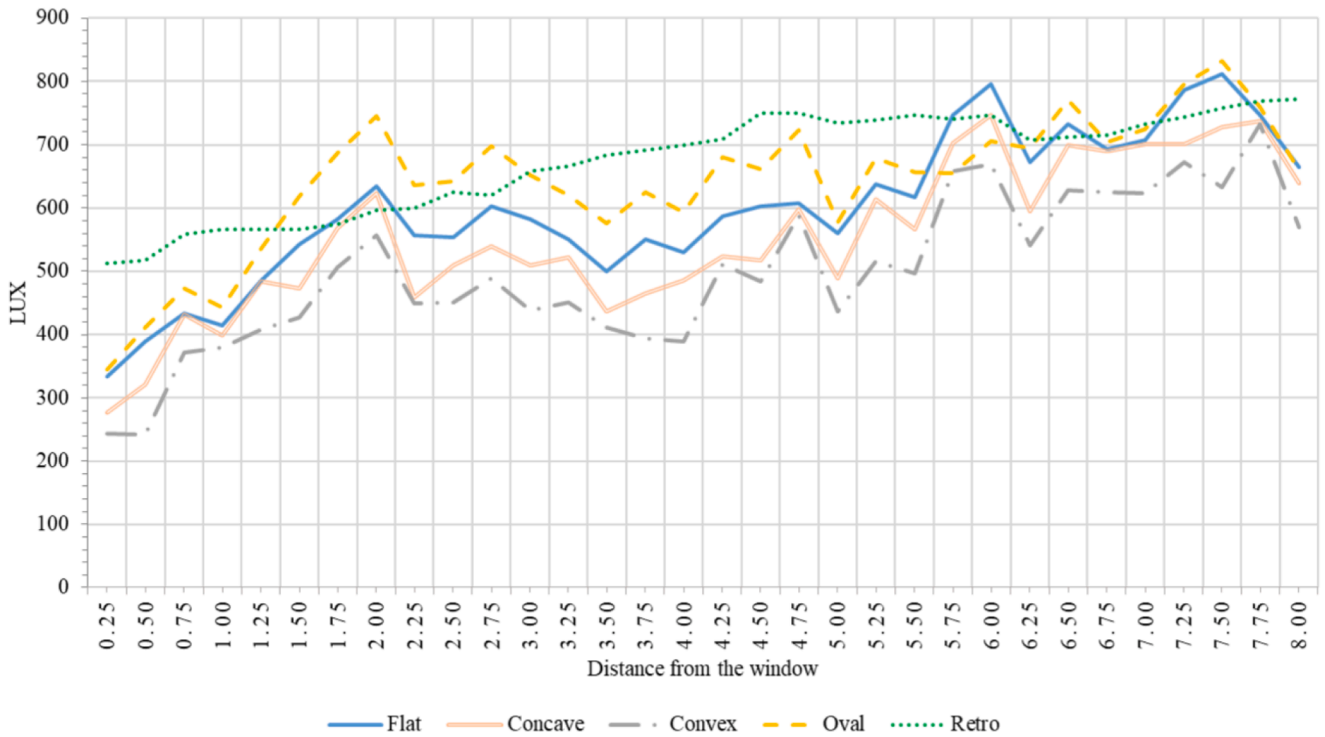
(a) Midline illuminance distribution at 12:00 on March 21st
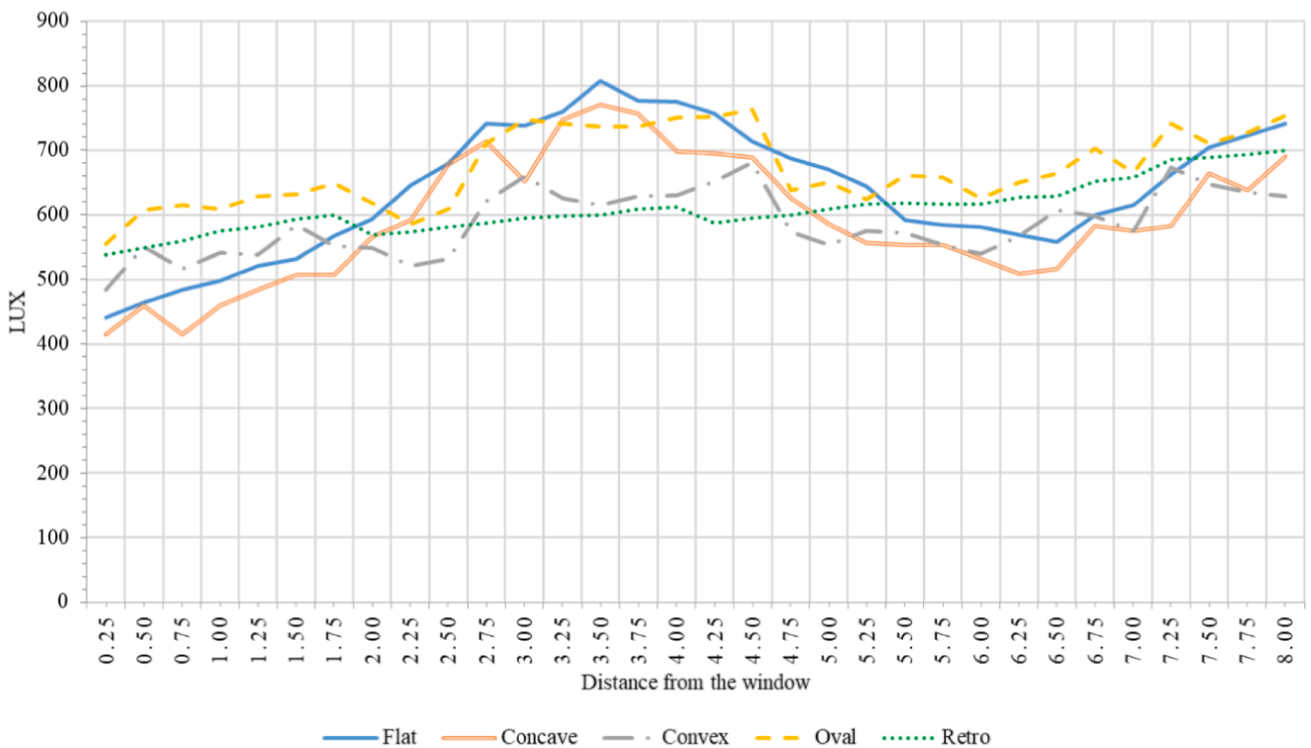
(b) Midline illuminance distribution at 12:00 on June 21st

Fig. 10. Illuminance distribution along the along the space midline for different types of slats in the upper section of the split louver at 12:00 on three typical dates.

In addition, the illuminance distribution maps in the workspace for the five types of slats at 8:00 and 10:00 on the three typical dates are presented in Fig. 8 and Fig. 9. The slat with a retro shape shows

noticeably better performance compared to other slats in the early morning (8:00) on December 21st with low solar angles. This is because it prevents light penetration between adjacent slats, leading to a peak

(c) Midline illuminance distribution at 12:00 on December 21st

Fig. 10. (*continued*).

(a) Flat
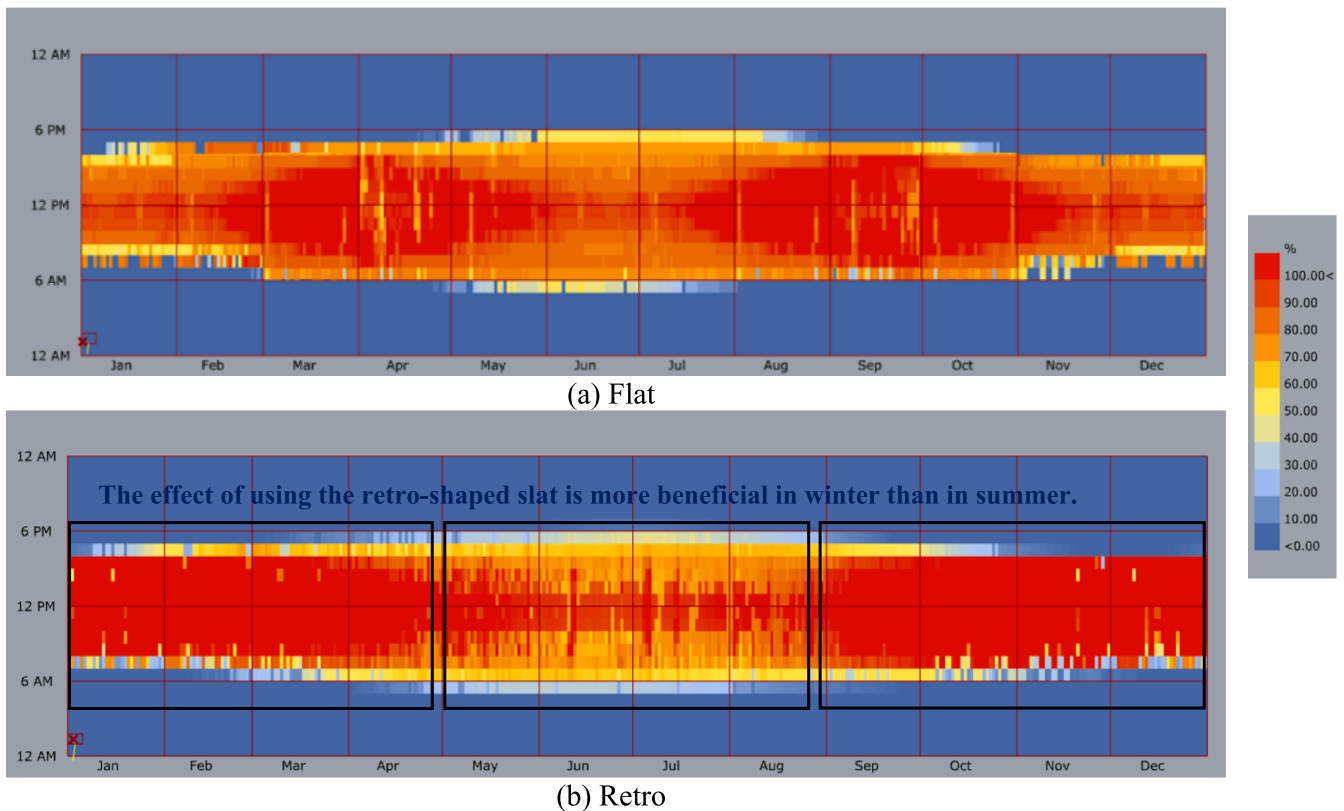
(b) Retro

Fig. 11. Annual daylighting coverage percentage within UDI$_{150 \sim 750 \text{ lx}}$ for two different slat shapes (flat and retro).

UDI$_{150 \sim 750 \text{ lx}}$ percentage (82 %). At all times, there are no light patches in the work plane when *retro*-shaped slats are applied, which means the blinds might not be required in this case. Therefore, an analysis without blinds is included in the discussion section.

As previously noted, highlighting the inconsistency in daylight distribution during the early morning and late afternoon hours is essential.

Therefore, the illuminance distribution through the work plane along the space midline between the window and the end wall (side cross-sectional) for different slat shapes at 12:00 on the three typical dates is further studied. The results are shown in Fig. 10.

Across various days, the slats exhibit consistent daylight distribution performance, regardless of average illuminance levels within the space.

(a) The illuminance along the space midline
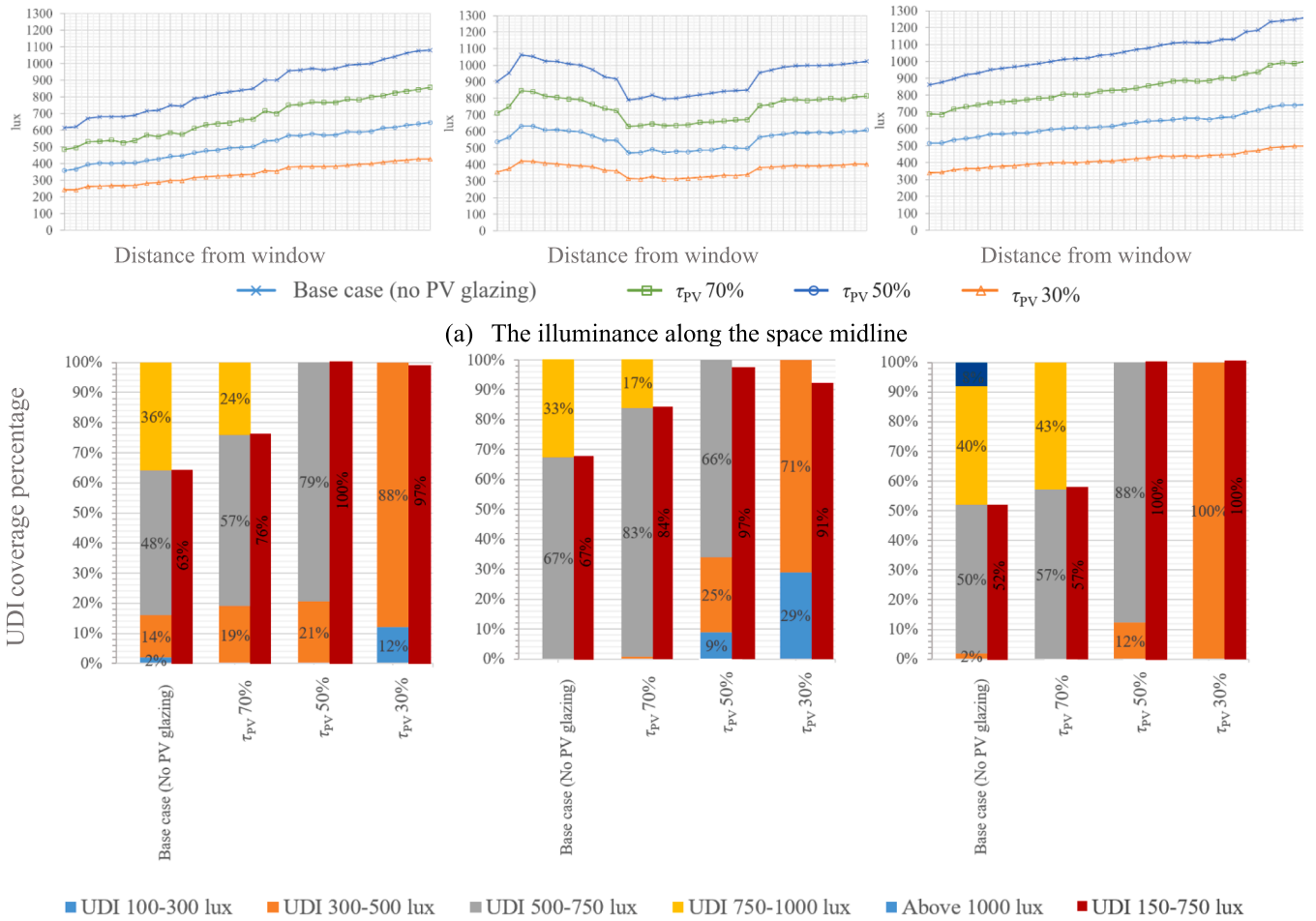
Fig. 12. The effect of PV glass transmittance (τ_PV of 70%, 50%, and 30%) on illuminance levels of the split louver with *retro*-shaped slats at 12:00 on three typical dates.

	08:00	10:00	12:00	08:00	10:00	12:00	08:00	10:00	12:00
		March 21st			June 21st			December 21st	
◇ Flat	0.35	0.60	0.60	0.60	0.60	0.60	0.20	0.20	0.55
+ Convex	0.45	0.65	0.65	0.60	0.60	0.50	0.20	0.20	0.60
△ Concave	0.45	0.66	0.63	0.60	0.60	0.50	0.20	0.20	0.50
✕ Oval	0.49	0.50	0.50	0.60	0.50	0.55	0.20	0.30	0.40
○ Retro	0.55	0.70	0.65	0.65	0.70	0.60	0.30	0.55	0.65
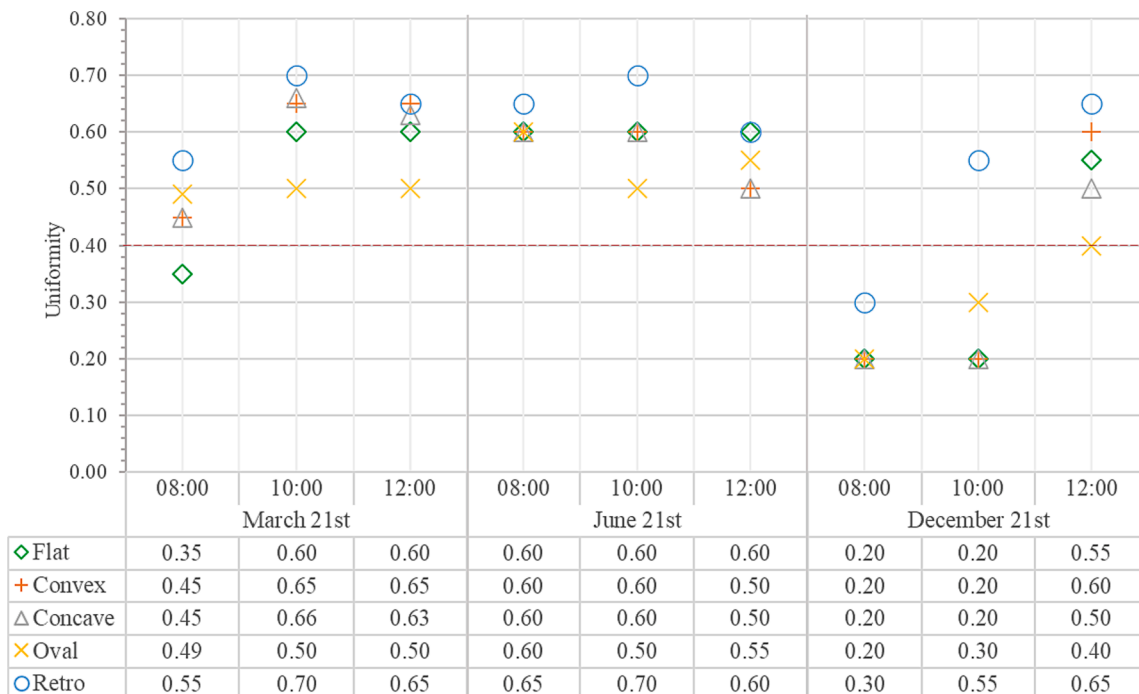
Fig. 13. The uniformity level for different types of slats at different times on three typical dates.

Base case (no PV glazing)	τ_{PV} 70%	τ_{PV} 50%	τ_{PV} 30%
0.31 Imperceptible glare	0.27 Imperceptible glare	0.24 Imperceptible glare	0.20 Imperceptible glare

(a) Glare maps at 12:00 on March 21st

	Base case (no PV glazing)	τ_{PV} 70%	τ_{PV} 50%	τ_{PV} 30%
— ✕ — March 21st	0.31	0.27	0.24	0.20
— ▢ — June 21st	0.24	0.20	0.16	0.13
— △ — December 21st	0.36	0.31	0.25	0.21
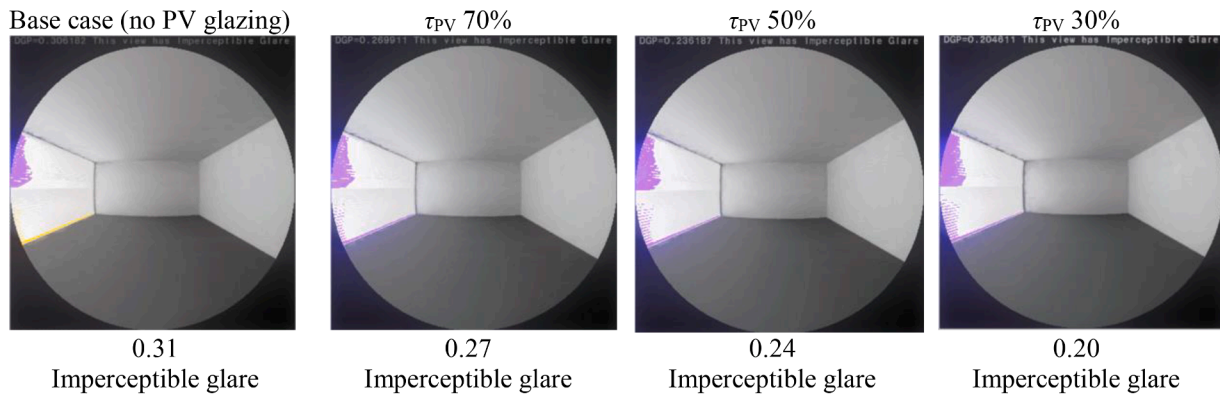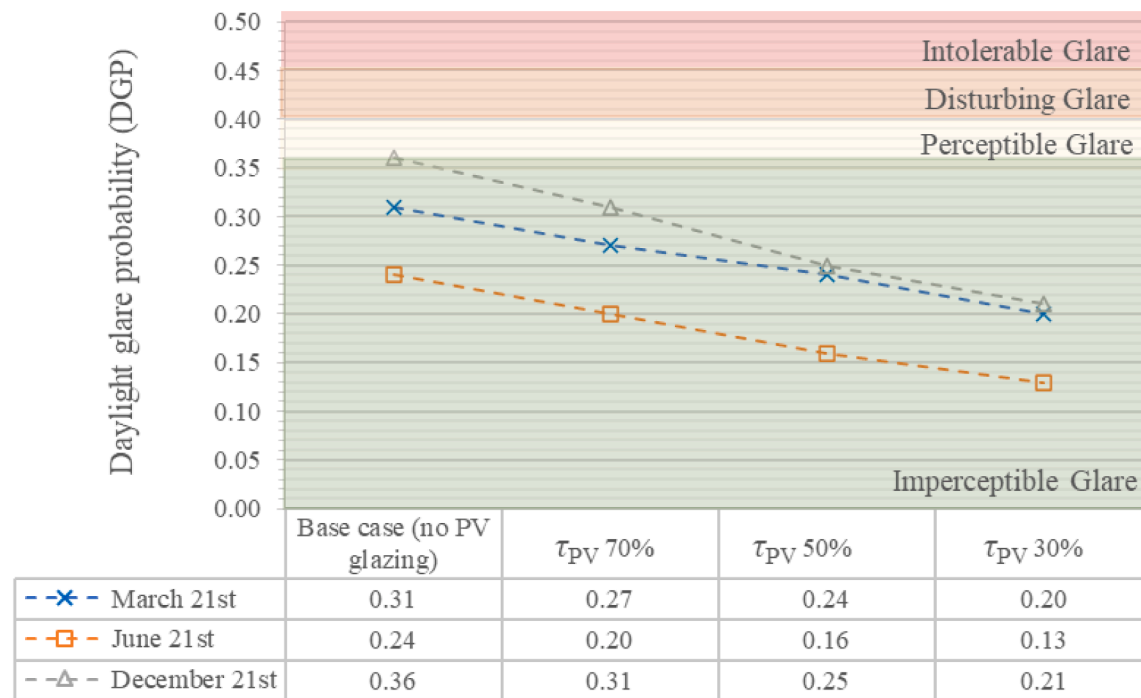
(b) Daylight Glare Probability (DGP) at 12:00 on three typical days

Fig. 14. The effect of PV glass transmittance (τ_{PV} of 70%, 50%, and 30%) on daylight glare of the split louver with *retro*-shaped slats at 12:00 on three typical dates.

Among the five slat types, illuminance values experience a significant rise on March 21st and December 21st, progressing from around 200–500 lx near the window to 600–800 lx on March 21st and from about 450–600 lx to 700–1000 lx on December 21st. Conversely, on June 21st, a more moderate increase is observed, spanning 400–600 lx to 630–700 lx, with a prominent peak in the room's middle reaching up to 800 lx. The flat and curved (convex and concave) slats showcase comparable daylight distribution, while the oval-shaped slat tends to concentrate illuminance closer to the window compared to other scenarios. Notably, the *retro*-shaped slat case displays considerably smaller illuminance variations along the midline, distinguishing it from flat, curved, and oval-shaped slats.

In terms of annual UDI performance (Fig. 11), the *retro*-shaped slat in the split louver exhibits heightened useful daylighting, as a greater percentage of working hours fall within the UDI150 ~ 750 lx range compared to the flat slat. This enhancement is particularly evident during winter, where most working hours achieve 100 % coverage.

3.1.2. Effect of PV glass transmittance

To explore the effect of the PV glass transmittance (τ_{PV}) in terms of daylight quantity, an analysis of UDI bin coverage percentages and the illuminance along the midline is conducted with consideration of the slat shape analysis in Section 3.1.1. The effect of different PV glass transmittances on the illuminance distribution along the space midline at 12:00 on the three typical dates using the *retro*-shaped slat is presented in Fig. 12(a). In addition, the percentage coverage of UDI bins on the three typical dates at 12:00 is illustrated in Fig. 12(b) for different PV glass transmittance cases, including the base case without the involvement of PV glazing.

For all three typical dates, the illuminance values consistently decrease with lower τ_{PV}. The UDI bins are also impacted because of the decreasing average illuminance. Acceptable coverage percentages of the recommended UDI bins (UDI$_{300\sim500\ lx}$ and UDI$_{500\sim750\ lx}$) for a certain range of τ_{PV} (50 % and 30 %) are achieved. The UDI$_{500\sim750\ lx}$ coverage increases in the cases of τ_{PV} 70 % and 50 %, with the value achieving 57 %-83 % and 66 %-88 %, respectively. In the case of τ_{PV} 30 %, the
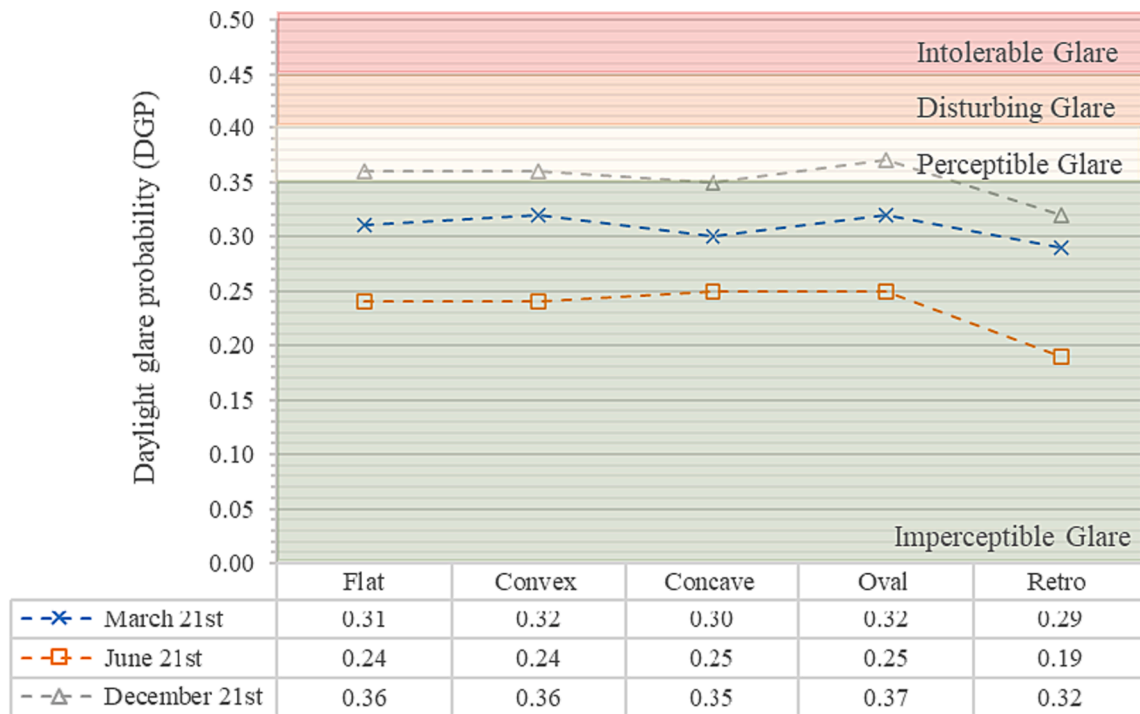
Fig. 15. Daylight Glare Probability (DGP) indices at 12:00 on three typical dates with different slat shapes.

	Flat	Convex	Concave	Oval	Retro
– ✳ – March 21st	0.31	0.32	0.30	0.32	0.29
– ☐ – June 21st	0.24	0.24	0.25	0.25	0.19
– △ – December 21st	0.36	0.36	0.35	0.37	0.32

$UDI_{300\sim500\ lx}$ shows significant percentages between 71 % and 100 % due to the lower transmitted daylight. Compared to the base case, the τ_{PV} 70 % case gives lower percentages of illuminance within $UDI_{750\sim1000\ lx}$ on March 21st and June 21st. On December 21st, however, the coverage percentage of $UDI_{750\sim1000\ lx}$ for the τ_{PV} 70 % case slightly increases from 40 % to 43 %. In Fig. 12(b), the $UDI_{150\sim750\ lx}$ percentage is the total of the $UDI_{100\sim300\ lx}$, $UDI_{300\sim500\ lx}$, and $UDI_{500\sim750\ lx}$, or slightly less when the percentage between 100 and 150 lx is excluded. It is clear that, with a τ_{PV} of 50 %, the $UDI_{150\sim750\ lx}$ percentage is the highest among the four PV glass transmittance cases.

3.2. Daylight quality analysis

3.2.1. Daylight spatial distribution: Daylight uniformity

The analysis of daylight distribution uniformity on the work plane for various slat types is carried out and illustrated in Fig. 13, regardless of the PV glass transmittance. For the three typical dates, the daylight spatial distribution of the *retro*-shaped slats is generally more uniform. In contrast, the oval-shaped slat achieves the minimum values of average uniformity, while flat- and curved-shaped slats show a similar trend. The *retro*-shaped slats give the best performance with an average uniformity of 0.59, followed by the convex (0.49), flat (0.48), and concave (0.48) shaped slats, and the oval-shaped slats provide the lowest average uniformity of 0.45. Referring to the illuminance maps shown in Section 3.1.1, the oval-shaped slat considerably concentrates light near the window, leading to a lower average uniformity level. The *retro*-shaped slat gives the highest values at different working hours on the three typical dates, with the maximum value reaching 0.70 at 10:00 on March 21st and June 21st. On the other hand, although the minimum uniformity for the *retro*-shaped slat (0.30, at 8:00 on December 21st) is lower than the recommended uniformity level (0.40), it performs noticeably better compared to the other slats, for whom the uniformity is only 0.2. This is because the *retro*-shaped slat is capable of preventing sunlight from passing through the area between adjacent slats in the early morning of December 21st, when the solar angle is quite low.

It is worth mentioning that the uniformity of the daylight distribution is unaffected by the variation of PV glass transmittance because the ratio of the minimum illuminance to the average illuminance is constant.

3.2.2. Daylight glare: Daylight glare probability

This section investigates the effect of PV glass transmittance (τ_{PV}) and slat shapes on daylighting performance through daylight glare studies. Glare is evaluated at the height of the eye level and in the direction of the viewer in a standing position at around 1.70 m above the floor.

Firstly, the PV glass at different transmittance values is studied using *retro*-shaped slats, and the results are shown in Fig. 14. Glare analysis in the work plane using Radiance maps at 12:00 on March 21st is presented along with DGP indices. On March 21st, the DGP indices are imperceptible in all cases (base case with no PV glazing involved and PV glazing with different transmittance values). Furthermore, the Radiance maps show that glare is minimised by using less PV glass transmittance, with values of 0.31, 0.27, 0.24, and 0.20 for the base case, τ_{PV} 70 %, τ_{PV} 50 %, and τ_{PV} 30 % cases, respectively. For the other two typical dates, the DGP comparison in the work plane at 12:00 also revealed that PV glass with all selected transmittance values gives acceptable ranges of perceptible and imperceptible glare.

Secondly, the glare performance of different slat shapes is evaluated. Fig. 15 illustrates the comparison among different types of slats in terms of the DGP in the work plane at 12:00 on the three typical dates. The effect of slat shape on glare probability is not as great as that of PV glass transmittance, although the *retro*-shaped slat obtains the most acceptable range of imperceptible glare on all three typical dates. Specifically, the average DGP of the *retro*-shaped slat is the lowest (0.26) among all slats, indicating its advantage in avoiding glare probability. In contrast, the oval-shaped slat gives an average DGP of 0.31, which is the highest among the studied cases. Besides, the flat- and curved-shaped slats perform similarly in reducing glare potential, with the average DGP being 0.3 for the three typical dates.
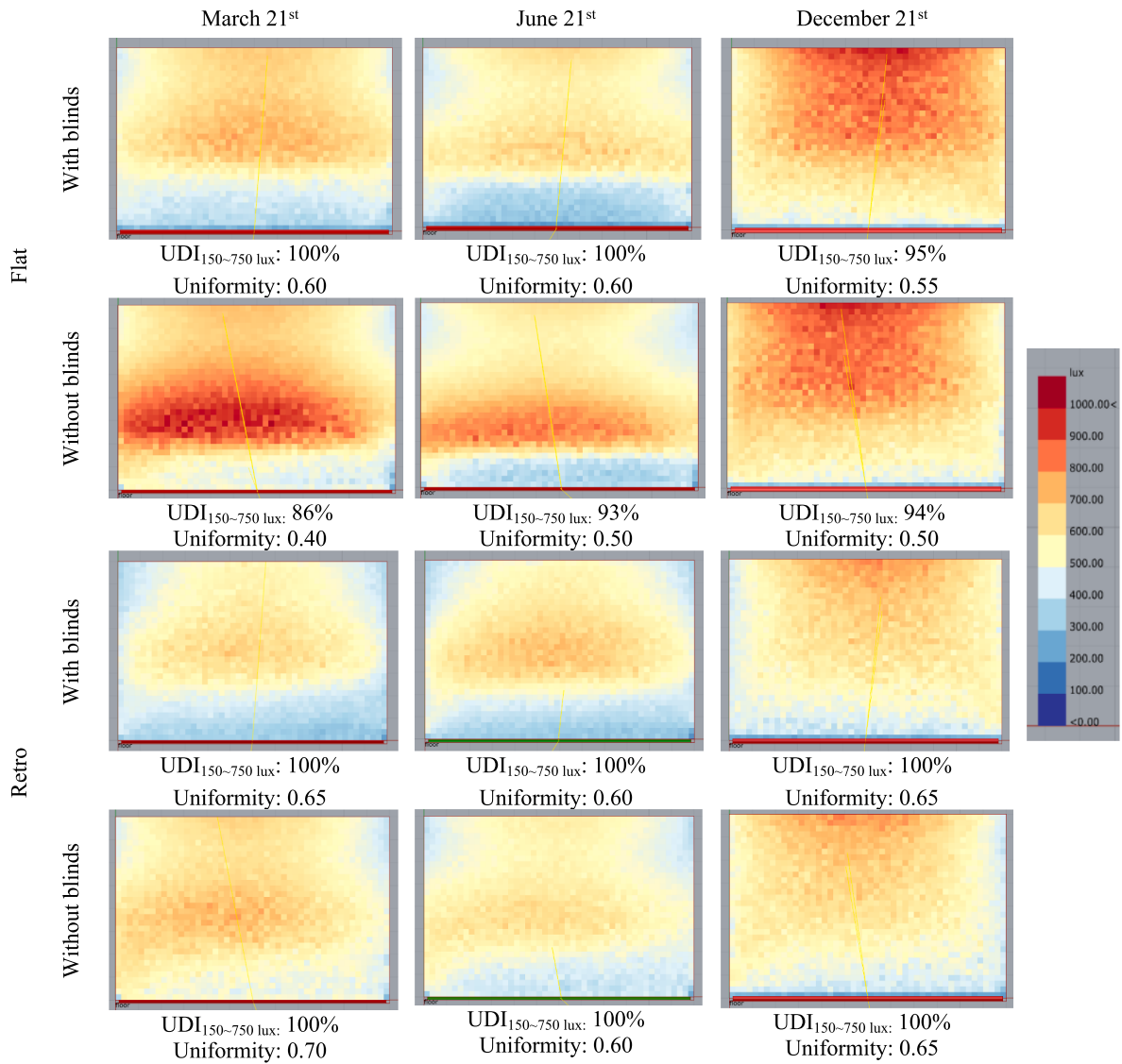
Fig. 16. Illuminance map comparison between two slat shapes (flat and retro) both with and without common blinds at 12:00 on three typical dates.

4. Discussions

4.1. Reliability and practicality of using the retro-shaped slat

Promoting any new daylighting system requires a focus on practical elements and a decrease in the system's component count to assure its design practicality. The role of the slat shape is discussed in the previous sections on daylighting quantity and quality. This section explores the application of the specially designed retro shape as a more reliable and practical slat configuration, with the added advantage of eliminating the need for an attached blind system. This approach consequently leads to a reduction in system weight, the attainment of a distinctive shape, and the elimination of superfluous system components. To demonstrate the advantages of the *retro*-shaped slat in eliminating the blind, its daylighting performance with and without the blind system is investigated and compared with that of the flat slat. The daylighting performance of the split louver is presented by using the illuminance maps in Fig. 16 and Fig. 17 for all three typical dates at 12:00 and 8:00, respectively. Most illuminance maps for the flat slat clearly show daylight patches when there is no blind used on all the typical dates, particularly at 8:00, with direct penetrating sunlight appearing on December 21st.

At noon, the impact of blinds on the illuminance distribution in the flat slat-based split louver is more pronounced than in the retro slat-based counterpart, as depicted in Fig. 16. Without the benefit of the blinds system, the $UDI_{150\sim750\ lx}$ and uniformity values in the flat slat case decreased from 100 % and 0.6 to 86 % and 0.4, respectively, on March 21st. However, provided the *retro*-shaped slat is applied, the $UDI_{150\sim750\ lx}$ still reaches 100 %, and the uniformity value even slightly increases from 0.65 to 0.70 on the same day, though the blinds are not involved.

Fig. 17 indicates that the daylighting performance at 8:00 is quite different from that at 12:00. In the case of the flat slat, the blinds assist in improving the $UDI_{150\sim750\ lx}$ and uniformity values up to 98 % and 0.40, respectively, on March 21st. However, in the case of the *retro*-shaped slat, the $UDI_{150\sim750\ lx}$ slightly decreases from 100 % to 92 % with a similar uniformity level of around 0.60 after equipping with the blinds. The *retro*-shaped slat helps prevent any potential penetration due to its parametric angles. For instance, at 8:00 on December 21st, the penetration light is noticeable if blinds are not equipped with the flat slat, which does not occur in the retro slat case.

The annual daylighting coverage percentage within $UDI_{150\sim750\ lx}$ for the *retro*-shaped slat with and without blinds is depicted in Fig. 18. It is also shown that the *retro*-shaped slats can be used for a longer period
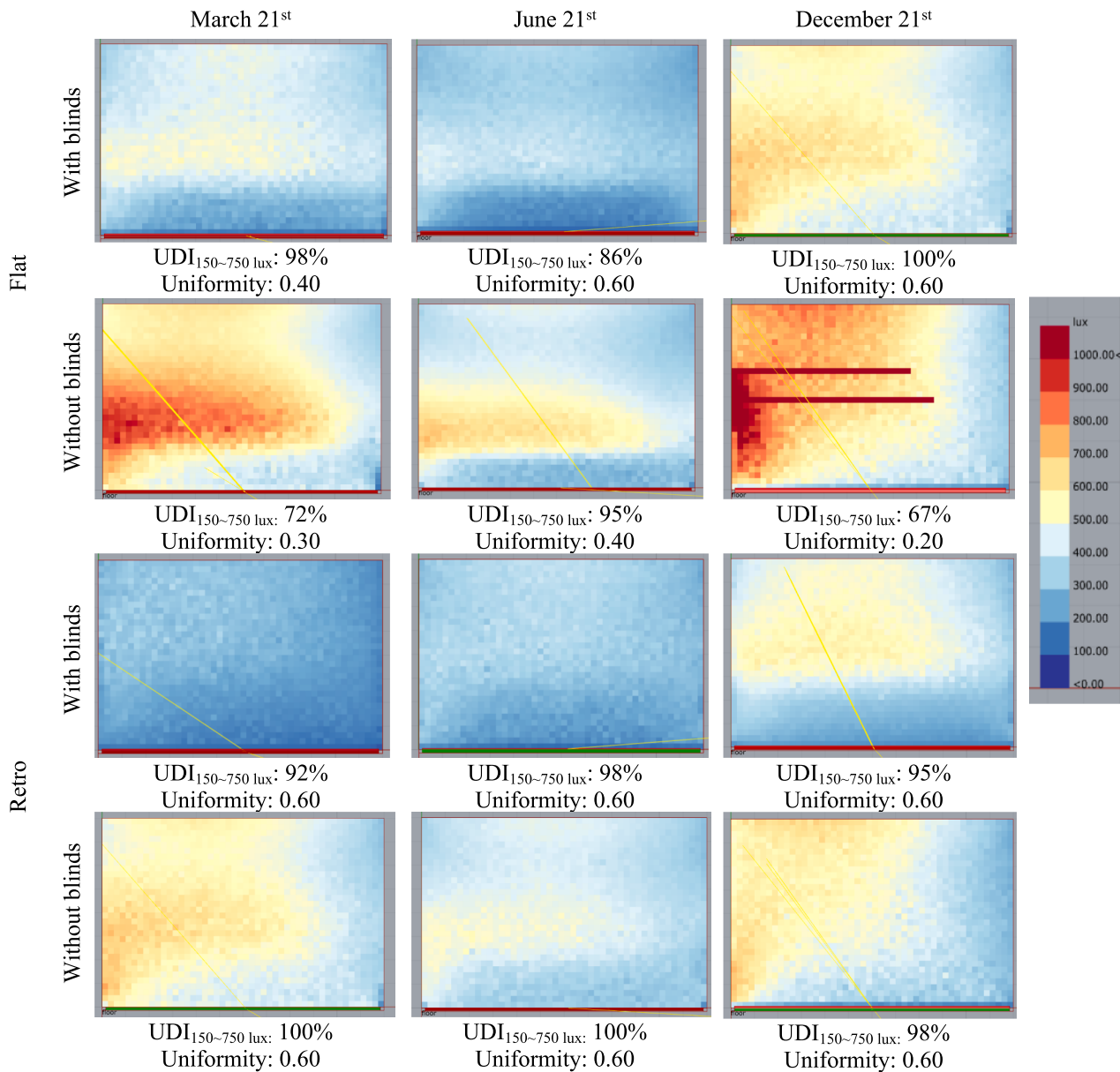
Fig. 17. Illuminance map comparison between two slat shapes (flat and retro) both with and without common blinds at 8:00 on three typical dates.

without blinds as an independent shading system. As shown, using *retro*-shaped slats without blinds increases the percentage of $UDI_{150\sim750\ lx}$ from around 60 % up to 100 % in the morning (around 9:00) from May to August and in the early morning (around 7:00) in March, April, and September compared to the *retro*-shaped slats with blinds.

4.2. Building energy implications of using the retro-shape slat

The design of the split louver system with parametrically incremental slat angles, incorporating the innovative *retro*-shaped slats, and considering the transmittance of PV glass, presents significant implications for building energy performance. This section delves into the building energy implications of the proposed design, taking into account the retro slat shape and PV glass transmittance.

(1) Daylighting and electric lighting demand:

The use of the split louver system with *retro*-shaped slats introduces a well-balanced daylighting strategy. The careful manipulation of slat angles optimizes daylight distribution, allowing ample natural illumination to penetrate deep into the interior spaces. This design minimizes the reliance on artificial lighting during daytime hours, leading to a reduction in electric lighting demand. The integration of the *retro*-shaped slats, which inherently provide superior daylight control compared to conventional flat slats, directly influences energy savings related to lighting.

(2) Photovoltaic glass transmittance and energy generation:

The consideration of photovoltaic (PV) glass transmittance as part of the design further enhances the building's energy profile. The integration of PV glass into the split louver system enables the conversion of incoming sunlight into electricity. The retro slat shape, with its meticulous parametric angles, synergistically interacts with the PV glass, optimizing the angle of incidence for solar energy capture. This integration contributes to on-site renewable energy generation, potentially offsetting a portion of the building's electricity demand.

(a) Retro-shaped slat with blinds

(b) Retro-shaped slat without blinds
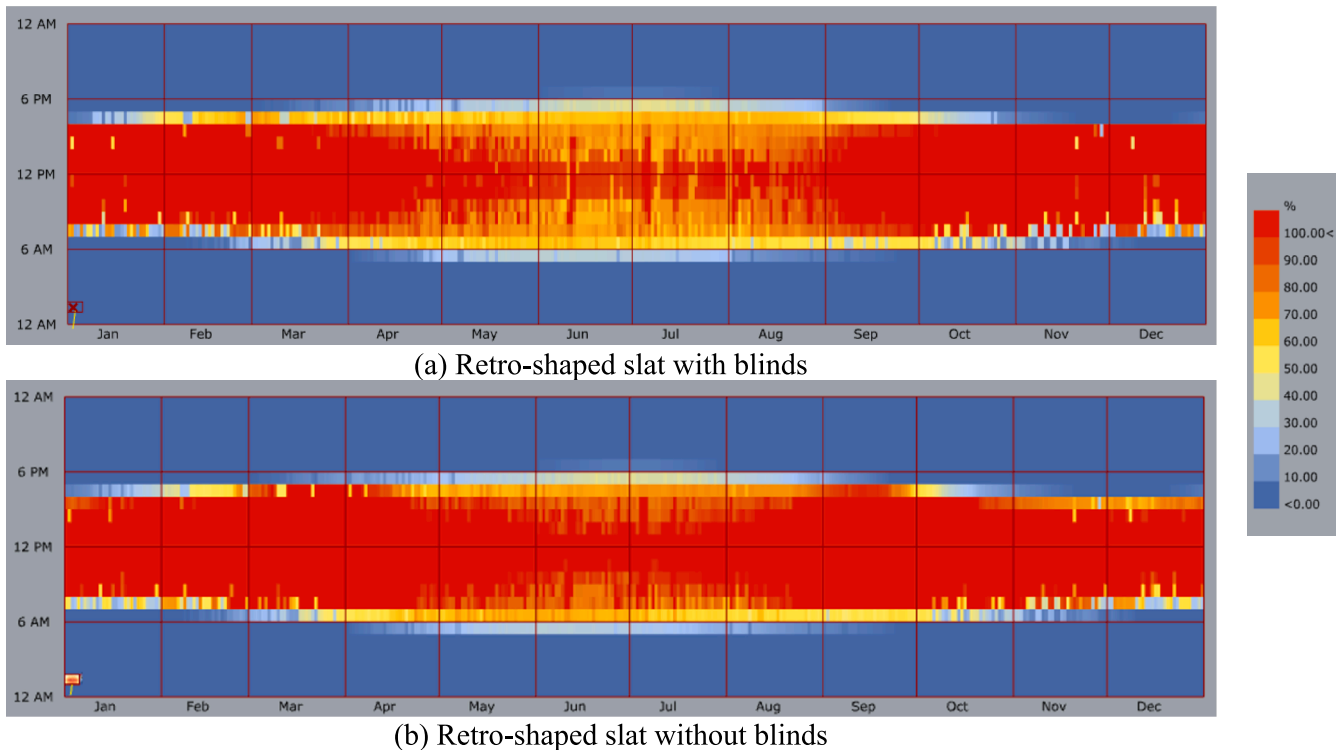
Fig. 18. Annual daylighting coverage percentage within UDI$_{150\sim750\ lx}$ of the *retro*-shaped slat with and without common blinds.

(3) Solar heat gain and cooling load reduction:

The *retro*-shaped slats play a pivotal role in managing solar heat gain within the building's interior. By parametrically adjusting the slat angles, the *retro*-shaped slats effectively prevent excessive penetration of direct sunlight during critical periods, such as early mornings and late afternoons. As a result, the cooling load on the building's HVAC system is substantially reduced. The shading effect of the *retro*-shaped slats, especially during peak cooling demand hours, contributes to lower energy consumption for air conditioning, thereby enhancing the overall energy efficiency of the building.

(4) Seasonal and geographical variability:

It's important to note that the building energy implications may exhibit variations based on geographical location and seasonal changes. The retro slat design, with its ability to adapt to different solar angles, proves particularly advantageous in regions with varying sunlight exposure throughout the year. The system's performance during specific seasons can be attributed to the retro slat shape's unique capabilities in managing solar penetration and daylight distribution.

Overall, the proposed split louver design with parametrically incremental retro slat angles and the integration of PV glass transmittance have substantial implications for building energy consumption and performance. By reducing solar heat gain, optimizing daylight distribution, and potentially contributing to renewable energy generation, this innovative design fosters a more sustainable overall energy performance.

5. Conclusion

This study introduces an innovative daylighting solution featuring a parametrically controlled split louver system integrated with PV glazing. The goal is to achieve consistent and uniformly distributed daylight throughout working hours in a deep-plan office space. The effect of different slat shapes and PV glass transmittance values on daylighting

performance is comprehensively evaluated, and the results help to draw the following conclusions:

(1) The slat shape has a greater effect on daylight level uniformity than on glare probability. The proposed design of the *retro*-shaped slat shows promising merit in providing relatively steady and distributed daylight coverage up to 100 % of the work plane area within the recommended acceptable range of 150 ~ 750 lx during working hours without using additional blinds. It also helps to achieve desired levels of uniformity up to 0.70.

(2) Different daylighting performance requirements are met by achieving acceptable coverage percentages of the recommended useful daylight illuminance (UDI) bins (UDI$_{300\sim500\ lx}$ and UDI$_{500\sim750\ lx}$) using PV glass transmittance values between 50 % and 30 %. Daylight glare is significantly influenced by PV glass transmittance values, and τ_{PV} of 50 % and 30 % can reduce daylight glare to acceptable levels on all studied typical dates.

(3) The optimum combination of the PV glazing and *retro*-shaped slats can be a solution to achieve a modified system of the PV glazing-integrated split louver. Generally, the retro slat shape in conjunction with a proper transmittance of the PV glass (between 50 % and 70 %) delivers better daylighting performance in terms of illuminance level, uniformity, and daylight glare probability.

(4) The integration of *retro*-shaped slats and PV glass transmittance in the parametric split louver system offers a holistic approach to enhancing building energy efficiency. This approach encompasses optimized daylighting, minimized cooling loads, renewable energy production, and alignment with sustainable architectural principles.

Declaration of Competing Interest

The authors declare that they have no known competing financial interests or personal relationships that could have appeared to influence the work reported in this paper.

References

[1] X. Zhang, S.-K. Lau, S.S.Y. Lau, Y. Zhao, Photovoltaic integrated shading devices (PVSDs): A review, Sol. Energy 170 (2018) 947–968.

[2] J. Peng, J. Yan, Z. Zhai, C.N. Markides, E.S. Lee, U. Eicker, X. Zhao, T.E. Kuhn, M. Sengupta, R.A. Taylor, Solar energy integration in buildings, Appl. Energy 264 (2020) 114740.

[3] Y. Tan, J. Peng, M. Wang, Y. Luo, A. Song, N. Li, Comfort assessment and energy performance analysis of a novel adjustable semi-transparent photovoltaic window under different rule-based controls, in: Building Simulation, Springer, 2023, pp. 1-19.

[4] K. Konis, S. Selkowitz, Effective daylighting with high-performance facades: emerging design practices, Springer, 2017.

[5] L.L. Fernandes, E.S. Lee, A. Thanachareonkit, S.E. Selkowitz, Potential annual daylighting performance of a high-efficiency daylight redirecting slat system, in, Building Simulation, Springer 14 (3) (2021) 495–510.

[6] L.i. Lan, S. Hadji, L. Xia, Z. Lian, The effects of light illuminance and correlated color temperature on mood and creativity, in, Building Simulation, Springer 14 (3) (2021) 463–475.

[7] A. Eltaweel, S. Yuehong, Using integrated parametric control to achieve better daylighting uniformity in an office room: A multi-Step comparison study, Energ. Buildings 152 (2017) 137–148.

[8] A. Eltaweel, Y. Su, M.A. Mandour, O.O. Elrawy, A novel automated louver with parametrically-angled reflective slats; design evaluation for better practicality and daylighting uniformity, Journal of Building Engineering 42 (2021) 102438.

[9] D.M. Le, D.Y. Park, J. Baek, P. Karunyasopon, S. Chang, Multi-criteria decision making for adaptive façade optimal design in varied climates: Energy, daylight, occupants' comfort, and outdoor view analysis, Build. Environ. 223 (2022), 109479.

[10] Y. Sun, K. Shanks, H. Baig, W. Zhang, X. Hao, Y. Li, B. He, R. Wilson, H. Liu, S. Sundaram, Integrated semi-transparent cadmium telluride photovoltaic glazing into windows: Energy and daylight performance for different architecture designs, Appl. Energy 231 (2018) 972–984.

[11] X. Liu, Y. Wu, Numerical evaluation of an optically switchable photovoltaic glazing system for passive daylighting control and energy-efficient building design, Build. Environ. 219 (2022), 109170.

[12] M. Chen, W. Zhang, L. Xie, B. He, W. Wang, J. Li, Z. Li, Improvement of the electricity performance of bifacial PV module applied on the building envelope, Energ. Buildings 238 (2021), 110849.

[13] A. Ghosh, S. Sundaram, T.K. Mallick, Colour properties and glazing factors evaluation of multicrystalline based semi-transparent Photovoltaic-vacuum glazing for BIPV application, Renew. Energy 131 (2019) 730–736.

[14] Q. Xuan, G. Li, Y. Lu, B. Zhao, X. Zhao, G. Pei, Daylighting characteristics and experimental validation of a novel concentrating photovoltaic/daylighting system, Sol. Energy 186 (2019) 264–276.

[15] A. Cannavale, G.E. Eperon, P. Cossari, A. Abate, H.J. Snaith, G. Gigli, Perovskite photovoltachromic cells for building integration, Energ. Environ. Sci. 8 (5) (2015) 1578–1584.

[16] X. Hong, F. Shi, S. Wang, X. Yang, Y. Yang, Multi-objective optimization of thermochromic glazing based on daylight and energy performance evaluation, in, Building Simulation, Springer 14 (6) (2021) 1685–1695.

[17] K. Kapsis, V. Dermardiros, A. Athienitis, Daylight performance of perimeter office façades utilizing semi-transparent photovoltaic windows: a simulation study, Energy Procedia 78 (2015) 334–339.

[18] A. Noback, L.O. Grobe, S. Wittkopf, Accordance of light scattering from design and de-facto variants of a daylight redirecting component, Buildings 6 (3) (2016) 30.

[19] I.A. Mashaly, K. Nassar, S.I. El-Henawy, M.W. Mohamed, O. Galal, A. Darwish, O. N. Hassan, A.M. Safwat, A prismatic daylight redirecting fenestration system for southern skies, Renew. Energy 109 (2017) 202–212.

[20] A. Eltaweel, Y. Su, Controlling venetian blinds based on parametric design; via implementing Grasshopper's plugins: A case study of an office building in Cairo, Energ. Buildings 139 (2017) 31–43.

[21] M. Mayhoub, Innovative daylighting systems' challenges: A critical study, Energ. Buildings 80 (2014) 394–405.

[22] H. Köster, Daylighting Controls, Performance, and Global Impacts, in: V. Loftness (Ed.), Sustainable Built Environments, Springer US, New York, NY, 2020, pp. 383–429.

[23] Y. Zhang, Multi-Slat Combination Blind of Up-Down-Movement Type, in, Google Patents (2013).

[24] M. Alsukkar, M. Hu, M. Gadi, Y. Su, A Study on Daylighting Performance of Split Louver with Simplified Parametric Control, Buildings 12 (5) (2022) 594.

[25] M. Alsukkar, M. Hu, A. Eltaweel, Y. Su, Daylighting performance improvements using of split louver with parametrically incremental slat angle control, Energ. Buildings 274 (2022) 112444.

[26] A. Eltaweel, Y. Su, Q. Lv, H. Lv, Advanced parametric louver systems with bi-axis and two-layer designs for an extensive daylighting coverage in a deep-plan office room, Sol. Energy 206 (2020) 596–613.

[27] Z.L. Rogers, M.J. Holtz, C.M. Clevenger, N.E. Digert, Mini-optical light shelf daylighting system, in, Google Patents (2004).

[28] N.E. Digert, M.J. Holtz, Mini-optical light shelf daylighting system, in, Google Patents (2002).

[29] T.E. Kuhn, Solar control: A general evaluation method for facades with venetian blinds or other solar control systems, Energ. Buildings 38 (6) (2006) 648–660.

[30] A. Tzempelikos, The impact of venetian blind geometry and tilt angle on view, direct light transmission and interior illuminance, Sol. Energy 82 (12) (2008) 1172–1191.

[31] H. Köster, Daylighting controls, performance and global impacts, Sustain, Built Environ. 1 (2013) 112–162.

[32] W. Xie, Y. Dai, R. Wang, K. Sumathy, Concentrated solar energy applications using Fresnel lenses: A review, Renew. Sustain. Energy Rev. 15 (6) (2011) 2588–2606.

[33] K. Kim, B.S. Kim, S. Park, Analysis of design approaches to improve the comfort level of a small glazed-envelope building during summer, Sol. Energy 81 (1) (2007) 39–51.

[34] R. Singh, I.J. Lazarus, V. Kishore, Effect of internal woven roller shade and glazing on the energy and daylighting performances of an office building in the cold climate of Shillong, Appl. Energy 159 (2015) 317–333.

[35] R. Schregle, The RADIANCE Photon Map Extension User Manual, (2016).

[36] A. Eltaweel, M.A. Mandour, Q. Lv, Y. Su, Daylight Distribution Improvement Using Automated Prismatic Louvre, Journal of Daylighting 7 (1) (2020) 84–92.

[37] J. Mardaljevic, Validation of a lighting simulation program under real sky conditions, Int. J. Light. Res. Technol. 27 (4) (1995) 181–188.

[38] J. Mardaljevic, Examples of climate-based daylight modelling, in: CIBSE National Conference, Citeseer, 2006, pp. 1-11.

[39] J. Mardaljevic, Daylight, indoor illumination and human behavior, (2009).

[40] C.T. Do, Y.-C. Chan, Development of a New Framework for Daylighting Simulation with Dynamic Shading Devices, (2018).

[41] S. Subramaniam, Daylighting simulations with radiance using matrix-based methods, Lawrence Berke-ley National Laboratory, 2017.

[42] Radsite-website, Setting rendering options, (2019), Available: https://www.radiance-online.org/archived/radsite/radiance/refer/Notes/rpict_options.html, Accessed: [July 11 2022].

[43] N. Skandalos, D. Karamanis, PV glazing technologies, Renew. Sustain. Energy Rev. 49 (2015) 306–322.

[44] F. De Luca, A. Sepúlveda, T. Varjas, Multi-performance optimization of static shading devices for glare, daylight, view and energy consideration, Build. Environ. 217 (2022), 109110.

[45] T. Miyazaki, A. Akisawa, T. Kashiwagi, Energy savings of office buildings by the use of semi-transparent solar cells for windows, Renew. Energy 30 (3) (2005) 281–304.

[46] C.E. de Normalisation, European standard EN 17037: 2018–daylight in buildings, European Committee for Standardization, Brussel, 2018.

[47] N. Baker, K. Steemers, Daylight design of buildings: a handbook for architects and engineers, Routledge, 2014.

[48] F. Sicurella, G. Evola, E. Wurtz, A statistical approach for the evaluation of thermal and visual comfort in free-running buildings, Energ. Buildings 47 (2012) 402–410.

[49] J.-H. Lee, J.W. Moon, S. Kim, Analysis of occupants' visual perception to refine indoor lighting environment for office tasks, Energies 7 (7) (2014) 4116–4139.

[50] A.D. Galasiu, J.A. Veitch, Occupant preferences and satisfaction with the luminous environment and control systems in daylit offices: a literature review, Energ. Buildings 38 (7) (2006) 728–742.

[51] Y. Sun, D. Liu, J.-F. Flor, K. Shank, H. Baig, R. Wilson, H. Liu, S. Sundaram, T. K. Mallick, Y. Wu, Analysis of the daylight performance of window integrated photovoltaics systems, Renew. Energy 145 (2020) 153–163.

[52] B. BSI, 12464-1: 2011 Light and lighting-Lighting of work places, Indoor work 40 places, (2011).

[53] E.C.f. Standardization, Light and lighting—lighting of work places—Part 1: indoor work places, BSI Standard Publication, page 10. EN, 12464 (2011).

[54] J. Wienold, Dynamic daylight glare evaluation, in: Proceedings of Building Simulation, Citeseer, 2009, pp. 944-951.

[55] K.R. Wagiman, M.N. Abdullah, M.Y. Hassan, N.H.M. Radzi, A new metric for optimal visual comfort and energy efficiency of building lighting system considering daylight using multi-objective particle swarm optimization, Journal of Building Engineering 43 (2021), 102525.